ISSN: 2710-0723

Freeze-Thaw Damage Constitutive Model of Composite Cementitious Modified Porous Concrete

Yuhang Qin, Jian Yin

School of Civil Engineering, Central South University of Forestry and Technology, Changsha 410004, PR China

Abstract

To systematically investigate the effects of composite cementitious modification on the mechanical performance evolution and damage behavior of porous concrete (PC) under freeze-thaw conditions, porous concrete systems with different modification levels were established, and freeze-thaw cycling and uniaxial compression tests were conducted. Based on the stress-strain curves, the mechanical response characteristics and damage evolution behavior of PC under freeze-thaw action were systematically analyzed. According to Lemaitre's strain equivalence principle and Weibull statistical distribution theory, a nonlinear damage constitutive model considering cumulative freeze-thaw damage was established. The results indicate that composite cementitious modification can significantly improve the compressive strength and mechanical stability of unfrozen PC, while the brittle failure characteristics become more pronounced with increasing modification level. With increasing freeze-thaw cycles, all PC specimens exhibited reductions in peak stress and elastic modulus, increases in peak strain, and gradual flattening of the descending branch, indicating enhanced deformation capacity at macroscopic failure. Among all groups, the specimen with moderate composite modification level exhibited the optimal balance between strength retention and freeze-thaw resistance, maintaining relatively high bearing capacity after 48 freeze-thaw cycles. The proposed constitutive model accurately described the stress-strain relationships of PC at different freeze-thaw stages. The predicted curves agreed well with the experimental results, and the fitting correlation coefficients (R^2) were all higher than 0.97. The damage variable exhibited an *J*-shaped growth trend with increasing strain and finally approached 0.8 near failure. The results of this study can provide theoretical support for freeze-thaw damage analysis and durability prediction of porous concrete structures in cold regions.

Keywords

Porous Concrete; Composite Cementitious Modification; Freeze-thaw Cycle; Stress-strain Curve; Damage Constitutive Model.

1. Introduction

Porous concrete (PC) is a porous construction material characterized by high porosity and interconnected pore structures, and has been widely used in sponge city construction, pavement engineering, and stormwater management systems [1-3]. Compared with ordinary concrete, PC is generally designed with little or no fine aggregate, resulting in a large number of interconnected pores and relatively weak interfacial transition zones (ITZs). Therefore, it is more susceptible to freeze-thaw damage in cold-region service environments [4]. During repeated freeze-thaw cycles, the freezing and thawing of pore water can easily induce internal microcrack propagation, interface debonding, and local structural deterioration, thereby leading to the degradation of mechanical properties and structural stability [5]. Consequently,

ISSN: 2710-0723

improving the mechanical stability and freeze-thaw resistance of porous concrete has become an important research topic.

At present, studies on the freeze-thaw durability and mechanical behavior of porous concrete mainly focus on pore structure optimization, interfacial performance improvement, and material damage evolution. Existing studies have shown that pore structure characteristics and interfacial transition zone conditions are the key factors governing freeze-thaw damage development in PC [6]. Optimizing aggregate gradation and pore structures can improve structural stability and delay crack propagation to some extent, while the incorporation of mineral admixtures and composite cementitious materials can improve the matrix structure and interfacial bonding properties, thereby enhancing crack resistance and freeze-thaw durability [7]. In addition, the influence of composite cementitious systems on the mechanical properties of PC exhibits obvious stage-dependent characteristics, and the strength development, deformation capacity, and damage evolution behavior vary under different modification levels [8].

Existing studies mainly focus on strength degradation, pore structure evolution, and durability evaluation of porous concrete, whereas relatively limited attention has been paid to the stress-strain response and constitutive relationship under freeze-thaw action [9]. Most existing freeze-thaw damage constitutive models were established for ordinary concrete and are difficult to accurately characterize the damage accumulation and mechanical response evolution of PC with highly interconnected pores and multiple weak interfaces. Freeze-thaw action not only causes internal microcrack propagation and elastic modulus degradation, but also changes the peak strain, descending branch characteristics, and failure behavior of PC [10]. Therefore, it is necessary to establish a constitutive model capable of describing the freeze-thaw damage characteristics of porous concrete.

Accordingly, porous concrete systems with different composite cementitious modification levels were prepared in this study, and freeze-thaw cycling tests together with uniaxial compression tests were conducted. The failure modes, stress-strain response characteristics, and damage evolution behavior of PC at different freeze-thaw stages were systematically analyzed. Based on Lemaitre's strain equivalence principle and Weibull statistical theory, a constitutive model considering cumulative freeze-thaw damage was established, and the evolution laws of model parameters and damage variables were further discussed. The proposed model can provide a reference for freeze-thaw damage analysis and durability evaluation of porous concrete structures in cold regions.

2. Materials and Methods

2.1. Materials

The coarse aggregate used in this study was limestone crushed stone with a particle size of 19-26.5 mm, supplied by Hunan Sandstone Industry Co., Ltd. The bulk density, apparent density, and crushing value were 1546 kg/m^3, 2716 kg/m^3, and 22.1%, respectively. Ordinary Portland cement (OPC) of grade P·O 42.5 was supplied by Hunan Pingtang Southern Cement Co., Ltd, with a 28-day compressive strength of 51.8 MPa. Calcined 200-mesh diatomite (DE) was provided by Runhuabang New Materials Technology Co., Ltd. Oxalic acid (OA) and ferric sulfate (FS), used as chemical admixtures, were supplied by Sinopharm Chemical Reagent Co., Ltd. A 540P high-performance polycarboxylate superplasticizer (SP) manufactured by Sika AG was used as the water reducer, with a water-reduction rate of 30%. The physical properties and chemical compositions of OPC, DE, OA, and FS are presented in Tables 1-3.

ISSN: 2710-0723

Table 1. Chemical compositions of OPC and DE (wt.%)

Raw materials	CaO	SiO_2	Al_2O_3	SO_3	Fe_2O_3	MgO	Na_2O
Cement	62.55	21.89	5.58	2.89	2.86	2.26	0.83
DE	—	≥85	≤3.35	—	≤1.3	—	—

Table 2. Physical properties of chemical admixtures

Name	Chemical formula	Molecular weight	Purity(%)	Physical appearance
OA	$C_2H_2O_4·2H_2O$	126.07	99.5	Colorless crystals
FS	$Fe_2(SO_4)_3·xH_2O$	399.88	21.4	Light yellow powder

Table 3. Properties of polycarboxylate superplasticizer

pH	Solid content(%)	Water content(%)	Density(g/cm^3)	Water-reducing rate(%)
5.67	40	60	1.41	30

2.2. Specimen Preparation and Test Methods

The mix proportion of PC was designed using the volumetric method, with the target effective porosity ranging from 20% to 30%, and a porosity value of 20% was adopted in the mix calculation. The “paste-coating method” was used for PC preparation. The preparation procedure was as follows: OA, FS, and water were first mixed to prepare the composite modification solution. Subsequently, OPC, DE, and SP were mixed to obtain the cementitious powder. The cementitious powder and composite modification solution were then added into a UJZ-15 mortar mixer and mixed for 90 s to prepare a uniform cement paste. Afterward, the crushed stone and cement paste were added into an HJW-60 concrete mixer and mixed for 2 min to obtain a homogeneous mixture. Finally, the mixture was cast into molds in three layers, and each layer was manually compacted using a vibrating rod to ensure compact edges and corners without obvious slurry segregation. After casting, the specimens were demolded after 24 h at room temperature and cured under standard curing conditions at a temperature of (20 ± 2) °C and relative humidity above 95% until the specified curing age.

The freeze-thaw tests were conducted according to the slow-freezing method specified in the Standard for Test Methods of Long-Term Performance and Durability of Ordinary Concrete (GB/T 50082-2024). Prism specimens with dimensions of 150 mm × 150 mm × 300 mm and cubic specimens with dimensions of 150 mm × 150 mm × 150 mm were used to evaluate the mechanical properties under different freeze-thaw cycles. The freeze-thaw failure criteria were defined as either a compressive strength loss of 25% or a mass loss rate of 5%. Once the specimens reached the failure criterion, the corresponding group was no longer subjected to further freeze-thaw cycles.

Mechanical property tests were carried out according to the Standard for Test Methods of Concrete Mechanical Properties (GB/T 50081-2019). The compressive strength of the 150 mm × 150 mm × 150 mm cubic specimens was measured using a TYA-2000E microcomputer-controlled constant-temperature compression testing machine. To obtain complete stress-strain curves, uniaxial compression tests were conducted on 150 mm × 150 mm × 300 mm prism specimens. Considering the large number of pores inside PC, three preloading cycles were applied before formal loading to reduce the influence of initial pore compaction on the test results. The preloading procedure was consistent with that used in the elastic modulus test. During the formal loading stage, a constant loading rate of 0.2 MPa/s was adopted, and the full stress-strain response of the specimens was recorded. The mix proportions of PC with different

ISSN: 2710-0723

composite modification levels are listed in Table 4, in which Group B was used as the control group.

Table 4. Mix proportions and basic properties of PC (Unit: kg/m^3)

No.	Aggregate	Cement	DE	Water	SP	OA	FS	28d compressive strength/MPa	Measured porosity/%
B	1533	438	—	110	—	—	—	7.9	25.6
A1	1533	443	38.5	120	1.44	2.4	2.4	11.2	24.2
A2	1533	443	38.5	120	1.44	6.0	6.0	13.5	23.7
A3	1533	443	38.5	120	1.44	9.6	9.6	14.7	23.5

3. Results and Discussion

3.1. Failure Patterns and Stress-Strain Curves of PC

3.1.1. Failure Patterns

Fig. 1 shows the uniaxial compression failure patterns of PC with different composite modification levels before and after freeze-thaw cycles. Before freeze-thaw cycles (Fig. 1(a), (c), (e), and (g)), all specimens mainly exhibited splitting failure dominated by longitudinal cracking, while the failure characteristics varied with the modification level. In Groups B and A1, cracks were relatively dispersed and accompanied by local block spalling, showing obvious brittle failure characteristics. In contrast, Groups A2 and A3 exhibited more concentrated crack distributions and more pronounced through-crack features, and the overall structural integrity of the specimens was relatively better. After freeze-thaw cycles (Fig. 1(b), (d), (f), and (h)), the failure degree of all specimens became significantly more severe. The number and width of surface cracks increased obviously, accompanied by more noticeable local mortar spalling, and the longitudinal propagation tendency of cracks along the loading direction became more evident. Among them, Groups A2 and A3 exhibited relatively larger deformation capacity during failure. The main cracks gradually propagated along the interfacial transition zone (ITZ) and interconnected with surrounding microcracks, forming relatively dense crack networks, while the overall structures still maintained a certain degree of integrity.

Overall, all PC specimens experienced a typical evolution process of "microcrack initiation-crack propagation-unstable failure" during uniaxial compression. Freeze-thaw action significantly aggravated internal microcrack development and interface deterioration, resulting in reduced bearing capacity and more severe structural damage. Appropriate composite cementitious modification could improve the overall structural stability of PC to some extent and delay crack propagation and structural instability.

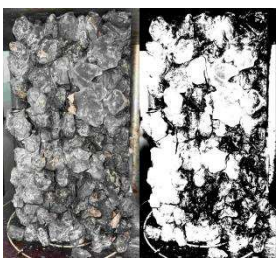

(a) B-0 cycles

(b) B-24 cycles

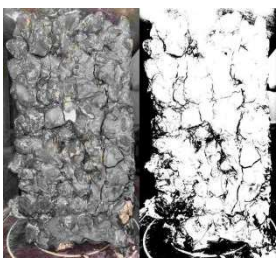

(c) A1-0 cycles

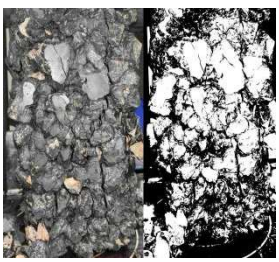

(d) A1-48 cycles

ISSN: 2710-0723

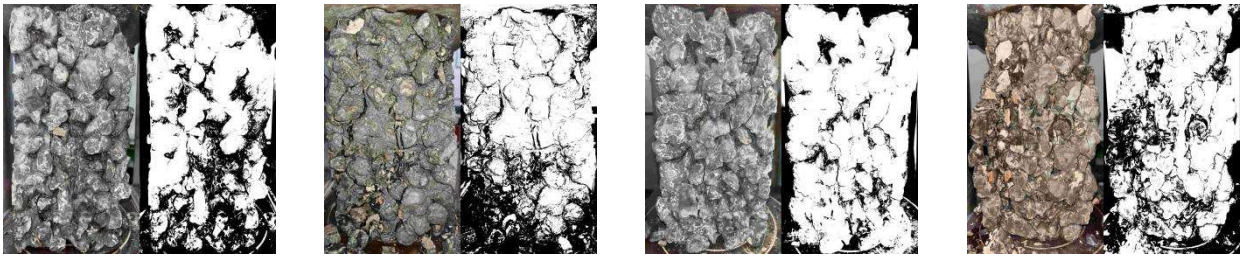

(e) A2-0 cycles (f) A2-48 cycles (g) A3-0 cycles (h) A3-36 cycles

Fig. 1 Failure patterns of PC with different composite modification levels before and after freeze-thaw cycles

3.1.2. Stress-Strain Curves

Fig. 2 presents the stress-strain curves of PC with different composite modification levels before freeze-thaw cycles, while Fig. 3 compares the stress-strain curves before and after freeze-thaw cycles. The corresponding mechanical parameters are listed in Table 5, where f_{cp} represents the peak stress, ε_p represents the peak strain, and E represents the elastic modulus.

As shown in Fig. 2, composite cementitious modification significantly improved the mechanical performance of PC. With increasing modification level, the peak stress of Groups A1, A2, and A3 increased by 52.17%, 72.46%, and 91.30%, respectively, compared with Group B, while the elastic modulus increased by 47.67%, 67.19%, and 76.15%, respectively. In contrast, the peak strain remained nearly unchanged at approximately 1.45×10^{-3}. The descending branches of all stress-strain curves were relatively steep, and the slope of the descending branch gradually increased with increasing modification level, indicating enhanced brittle failure characteristics and more concentrated failure behavior.

As shown in Fig. 3, the stress-strain curves of all PC specimens changed significantly with increasing freeze-thaw cycles, generally exhibiting the evolution characteristics of "peak reduction-curve flattening-deformation enhancement". The peak stress and elastic modulus continuously decreased, whereas the peak strain and ultimate strain gradually increased. After 24 freeze-thaw cycles, Group B reached the freeze-thaw failure state, and its peak stress decreased by 30.43% compared with the unfrozen condition, while the peak strain increased by 23.13%. After 36 freeze-thaw cycles, the peak stress reduction of Group A3 reached 36.36%, which was significantly higher than those of Groups A1 and A2 during the same stage. Meanwhile, the increase in peak strain of Group A3 was also greater than that of the other groups. After 48 freeze-thaw cycles, Groups A1 and A2 still maintained relatively high bearing capacities, among which Group A2 exhibited a relatively smaller reduction in peak stress, indicating better freeze-thaw stability.

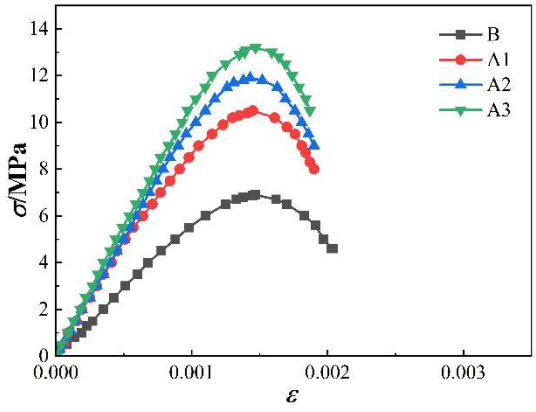

Fig. 2 Stress-strain curves of PC with different composite modification levels before freeze-thaw cycles

ISSN: 2710-0723

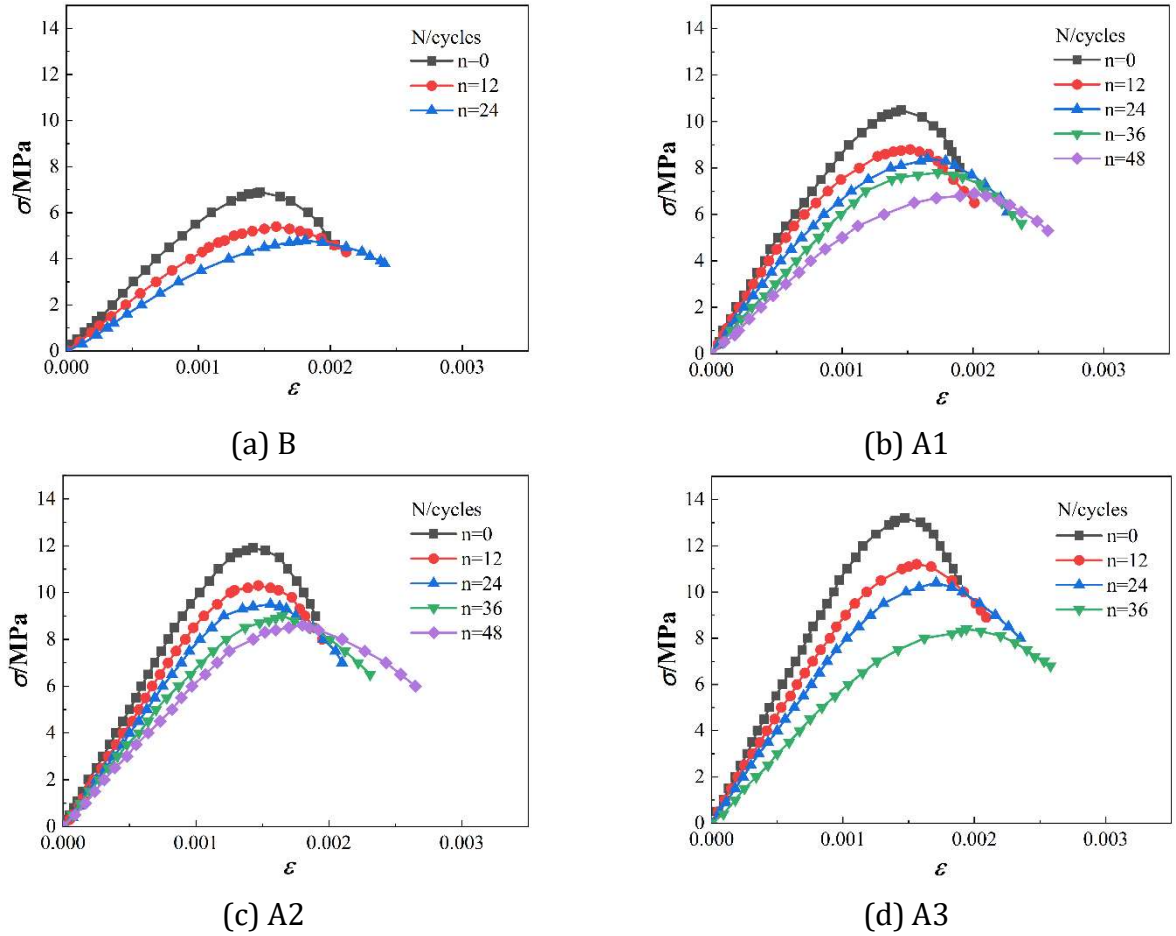

Fig. 3 Stress-strain curves of PC with different composite modification levels before and after freeze-thaw cycles

Table 5. Characteristic parameters of stress-strain curves of PC specimens before and after freezing and thawing

No.	Characteristic parameters	Freeze-thaw cycles				
		0	12	24	36	48
B	f_{cp}/MPa	6.9	5.4	4.8	—	—
	ε_p	1.47×10^{-3}	1.59×10^{-3}	1.81×10^{-3}	—	—
	E/MPa	6566	4918	4039	—	—
A1	f_{cp}/MPa	10.5	8.8	8.4	7.8	6.9
	ε_p	1.45×10^{-3}	1.52×10^{-3}	1.65×10^{-3}	1.73×10^{-3}	2.01×10^{-3}
	E/MPa	9696	8543	7433	6708	5889
A2	f_{cp}/MPa	11.9	10.3	9.5	9.0	8.6
	ε_p	1.43×10^{-3}	1.47×10^{-3}	1.56×10^{-3}	1.65×10^{-3}	1.80×10^{-3}
	E/MPa	10978	9903	8817	8019	7299
A3	f_{cp}/MPa	13.2	11.2	10.4	8.4	—
	ε_p	1.47×10^{-3}	1.56×10^{-3}	1.71×10^{-3}	1.94×10^{-3}	—
	E/MPa	11566	10257	9001	7067	—

The results indicate that appropriate composite cementitious modification can effectively improve the freeze-thaw damage resistance of PC and delay the occurrence of critical freeze-thaw failure. Among all groups, Group A2 exhibited better deformation capacity and freeze-thaw stability while maintaining relatively high strength. Although Group A3 exhibited

ISSN: 2710-0723

relatively high initial strength, its mechanical performance deteriorated more rapidly during the later freeze-thaw stage, indicating that excessive modification levels may adversely affect structural stability.

3.2. Establishment of Freeze-Thaw Damage Constitutive Model

3.2.1. Model Establishment

Based on Lemaitre's strain equivalence hypothesis [11], the strain generated in a damaged material under nominal stress can be regarded as equivalent to that generated in an undamaged material under effective stress. Therefore, the damage constitutive relationship of PC under freeze-thaw action can be expressed as:

$$\sigma = E_0 \varepsilon (1 - D) \tag{1}$$

where σ is the stress after n freeze-thaw cycles (MPa); E_0 is the initial static elastic modulus of PC (MPa); D is the total damage variable; and ε is the strain.

Under the combined effects of freeze-thaw cycles and external loading, the damage of PC can be considered as the coupling of freeze-thaw damage and loading damage. The total damage variable D satisfies the linear superposition principle:

$$D = D_c + D_n - D_c D_{\mathrm{n}} \tag{2}$$

where D_{c} is the damage variable caused by external loading, and D_{n} is the damage variable after n freeze-thaw cycles.

According to Weibull statistical distribution theory [12], assuming that the strength of material microelements follows the Weibull distribution, the loading damage variable D_{c} can be expressed as:

$$D_c = \left\{ 1 - \exp\left[-\left(\frac{\varepsilon}{a} \right)^b \right] \right\} \tag{3}$$

where a and b are the scale parameter and shape parameter of the Weibull distribution, respectively.

Based on continuous damage mechanics theory, the freeze-thaw damage variable D_{n} can be expressed as:

$$D_n = 1 - \frac{E_n}{E_0} \tag{4}$$

where E_{n} is the static elastic modulus of PC after n freeze-thaw cycles (MPa).

Therefore, the total damage variable D of PC under the combined effects of freeze-thaw cycles and external loading can be expressed as:

$$D = 1 - \frac{E_n}{E_0} \exp\left[-\left(\frac{\varepsilon}{a} \right)^b \right] \tag{5}$$

ISSN: 2710-0723

Combining Eqs. (1)-(5), the uniaxial compression damage constitutive equation of PC under freeze-thaw action can be obtained as:

$$\sigma = E_n \varepsilon \exp\left[-\left(\frac{\varepsilon}{a}\right)^b\right] \tag{6}$$

3.2.2. Analysis of Model Parameters

Fig. 4 illustrates the influence of parameters a and b on the stress-strain curves of PC under a constant equivalent elastic modulus E_n.

When parameter *b* remained unchanged, increasing parameter *a* caused relatively small changes in the overall curve shape, while both the peak stress and corresponding peak strain gradually increased. In contrast, when parameter *a* remained unchanged, increasing parameter *b* significantly increased the slope of the descending branch, accelerated the post-peak stress drop, and resulted in more obvious brittle failure characteristics.

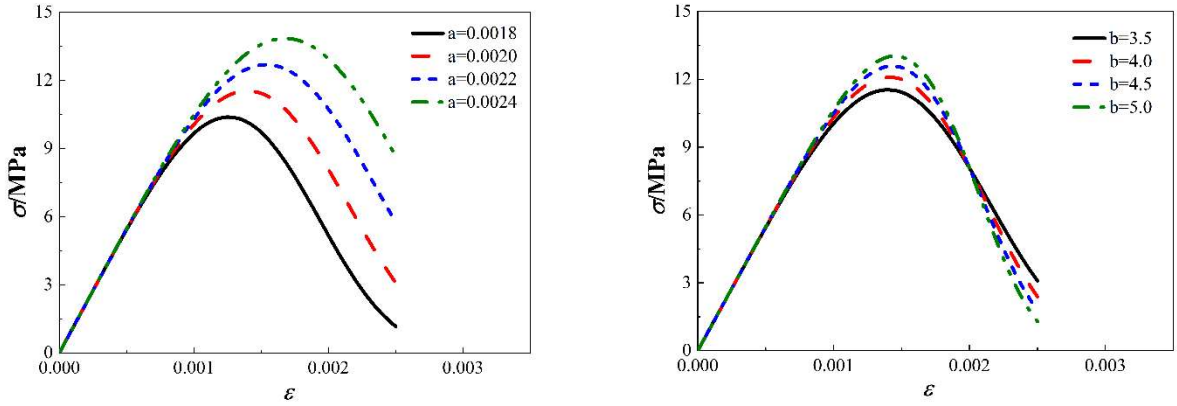

(a) Stress-strain curves with different values of parameter *a*

(b) Stress-strain curves with different values of parameter *b*

Fig. 4 Effect of parameters a and b on stress-strain curves of PC

3.2.3. Parameter Determination and Model Verification

By substituting the peak point (σ_p, ε_p) into Eq. (6) and combining the extremum condition at the peak point, the expressions of parameters a and b can be obtained as:

$$a = \frac{\varepsilon_p}{\left(\frac{1}{b}\right)^{\frac{1}{b}}}, b = \frac{1}{\ln\left(\frac{\varepsilon_p E_n}{\sigma_p}\right)} \tag{7}$$

Based on the experimental data listed in Table 5, nonlinear fitting of the stress-strain curves for PC with different composite modification levels was conducted using Eq. (6), and the corresponding constitutive model parameters are listed in Table 6.

The results indicate that parameter *a* gradually increased, whereas parameter *b* gradually decreased with increasing freeze-thaw cycles. This suggests that the peak strain of PC gradually increased after freeze-thaw action, while the descending branch became flatter, indicating weakened macroscopic instability characteristics.

Compared with the unfrozen state, under the ultimate freeze-thaw condition, parameter *a* of Groups B, A1, A2, and A3 increased by 24.75%, 27.58%, 24.75%, and 28.50%, respectively, while parameter *b* decreased by 25.35%, 38.13%, 33.76%, and 48.73%, respectively. These

ISSN: 2710-0723

results are generally consistent with the variation characteristics of the stress-strain curves shown in Fig. 3.

Further regression analysis between the model parameters and freeze-thaw cycles was conducted, and the evolution laws are presented in Fig. 5. Fig. 6 compares the predicted curves with the experimental curves. The results show that the predicted curves agree well with the experimental results, and all fitting correlation coefficients (R^2) are higher than 0.97, indicating that the proposed model can accurately describe the stress-strain relationships of PC with different composite modification levels under freeze-thaw action.

Table 6. Related parameters of constitutive model

No.	a	b	R^2
B-0 cycles	0.00202	3.183	0.988
B-12 cycles	0.00226	2.586	0.991
B-24 cycles	0.00252	2.376	0.986
A1-0 cycles	0.00203	3.496	0.991
A1-12 cycles	0.00205	3.058	0.990
A1-24 cycles	0.00228	2.952	0.989
A1-36 cycles	0.00241	2.637	0.988
A1-48 cycles	0.00259	2.163	0.978
A2-0 cycles	0.00202	3.492	0.993
A2-12 cycles	0.00207	3.191	0.987
A2-24 cycles	0.00215	3.078	0.981
A2-36 cycles	0.00230	2.647	0.987
A2-48 cycles	0.00252	2.313	0.988
A3-0 cycles	0.00207	3.893	0.988
A3-12 cycles	0.00222	2.651	0.984
A3-24 cycles	0.00241	2.485	0.985
A3-36 cycles	0.00266	1.996	0.976

Note: B-0 cycles represents Group B specimens subjected to 0 freeze-thaw cycles.

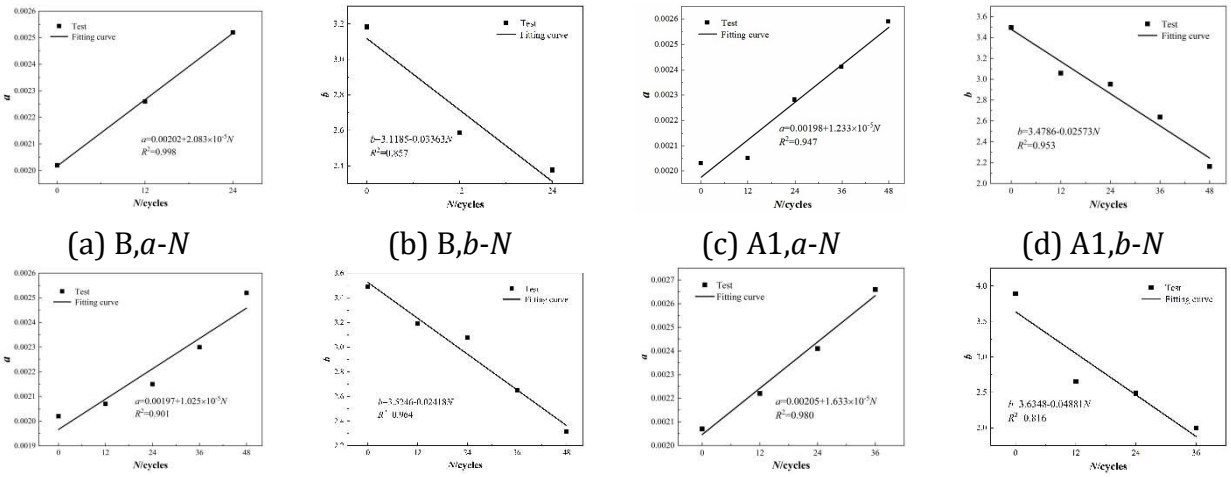

(a) B,a-N (b) B,b-N (c) A1,a-N (d) A1,b-N

(e) A2,a-N (f) A2,b-N (g) A3,a-N (h) A3,b-N

Fig. 5 Relationship between Weibull distribution parameters and freeze-thaw cycles of PC

ISSN: 2710-0723

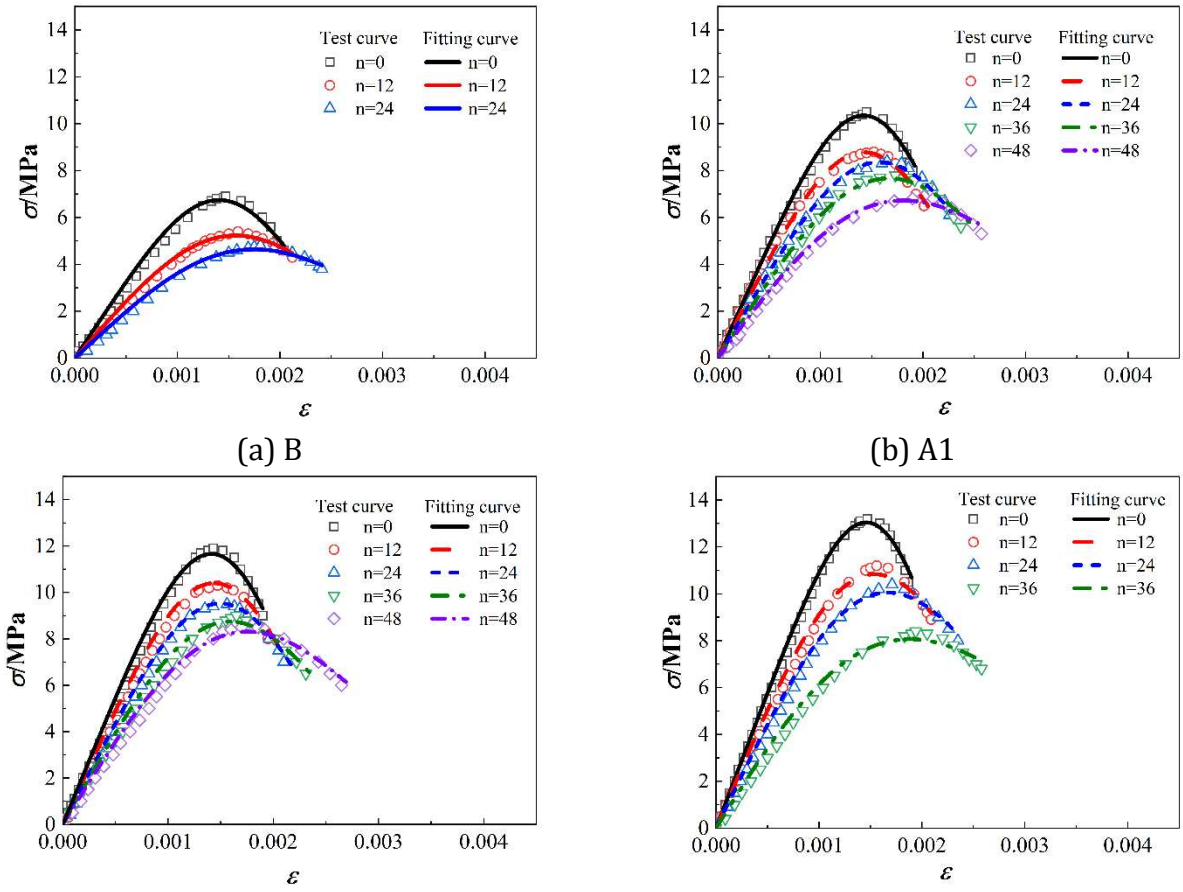

Fig. 6 Comparison between experimental and predicted stress-strain curves of PC with different composite modification levels before and after freeze-thaw cycles

3.2.4. Evolution of Damage Variables

According to Eq. (5), the damage variable *D* of each PC group was calculated, and the damage evolution curves under different freeze-thaw cycles are shown in Fig. 7.

As shown in Fig. 7, under different freeze-thaw stages, the damage variable *D* of all PC groups exhibited an *J*-shaped monotonic increasing trend with increasing strain and finally approached 0.8. According to the damage evolution characteristics, the process can be divided into a slow damage stage and a rapid damage stage. During the slow damage stage, the curve slope remained relatively small and the damage growth rate was relatively low, indicating that only a limited number of unconnected microcracks were generated inside the PC. With increasing freeze-thaw cycles, the initial damage value corresponding to zero strain gradually increased, indicating continuous accumulation of internal damage caused by freeze-thaw action. During the rapid damage stage, the curve slope increased significantly, and the growth rate of damage variable *D* increased rapidly, accompanied by the rapid increase in crack quantity and propagation range. As the strain approached the peak strain, internal microcracks rapidly propagated and gradually interconnected, eventually forming localized failure zones and resulting in overall structural instability.

Unlike ordinary concrete, which generally fails when *D* approaches 1, PC exhibited instability during the rapid growth stage of *D*, indicating more obvious damage localization characteristics. With increasing freeze-thaw cycles, the damage threshold corresponding to failure gradually increased, suggesting weakened macroscopic instability characteristics and enhanced deformation capacity at failure.

ISSN: 2710-0723

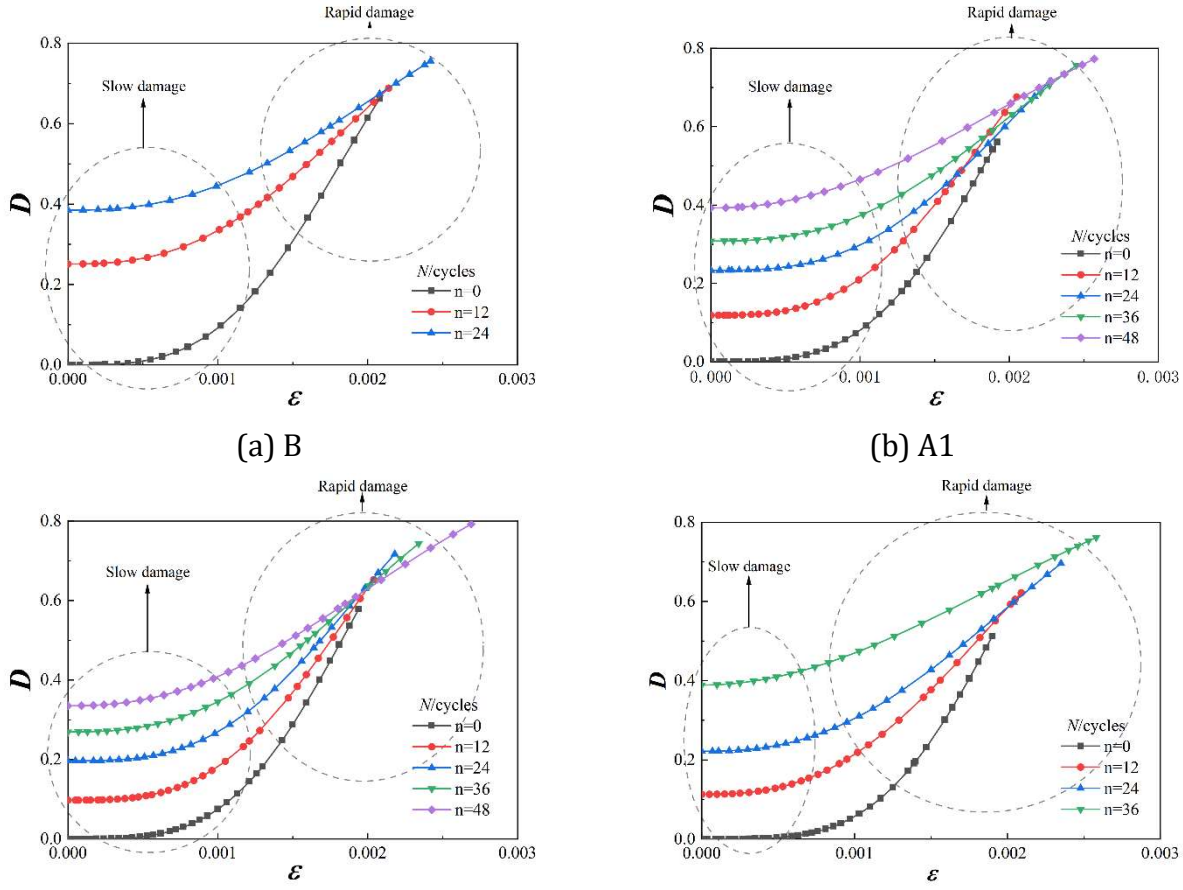

Fig. 7 Relationship between total damage variable *D* and strain *ε* of PC under different freeze-thaw cycles

4. Conclusion

(1) The uniaxial compression failure of PC was mainly characterized by splitting failure dominated by longitudinal cracking. With increasing composite modification level, the crack distribution became more concentrated and the overall structural integrity of the specimens improved, while the brittle failure characteristics became more pronounced. Freeze-thaw action significantly aggravated internal microcrack propagation and interface deterioration, resulting in increased crack quantity and width as well as gradual reduction in bearing capacity.

(2) Composite cementitious modification significantly improved the mechanical properties of PC. With increasing modification level, the peak stress and elastic modulus of all PC groups increased obviously, while the slope of the descending branch gradually increased. With increasing freeze-thaw cycles, all PC groups exhibited continuous reductions in peak stress and elastic modulus, gradual increases in peak strain, and flattening of the descending branch. Among all groups, Group A2 exhibited the best strength retention and freeze-thaw stability, whereas Group A3 showed relatively faster performance degradation during the later freeze-thaw stage.

(3) The freeze-thaw damage constitutive model established based on Lemaitre's strain equivalence principle and Weibull statistical theory could accurately describe the stress-strain relationships of PC at different freeze-thaw stages. The predicted curves agreed well with the experimental results, and all fitting correlation coefficients (R^2) were higher than 0.97. With increasing freeze-thaw cycles, parameter *a* gradually increased, whereas parameter *b* gradually

ISSN: 2710-0723

decreased, reflecting the gradual increase in peak strain and the weakening of macroscopic instability characteristics of PC.

(4) The damage variable *D* of all PC groups exhibited an *J*-shaped monotonic increasing trend with increasing strain and finally approached 0.8. With increasing freeze-thaw cycles, the initial damage value gradually increased, indicating the continuous accumulation of internal damage caused by freeze-thaw action. Meanwhile, PC exhibited structural instability during the rapid growth stage of the damage variable, showing obvious damage localization characteristics.

Acknowledgments

The author would like to acknowledge the National Natural Science Foundation of China(No. 52178262), the Science and Technology Innovation Program of Hunan Province (No.2020RC4049).

References

[1] Cui, X., Zhang, J., Huang, D., et al. (2017). Experimental study on the relationship between permeability and strength of pervious concrete. Journal of Materials in Civil Engineering, 29(11), 04017217.

[2] Xiang, J., Liu, H., Lu, H., et al. (2022). Degradation mechanism and numerical simulation of pervious concrete under salt freezing-thawing cycle. Materials, 15(9), 3054.

[3] Taheri, B. M., Ramezanianpour, A. M., Sabokpa, S., et al. (2021). Experimental evaluation of freeze-thaw durability of pervious concrete. Journal of Building Engineering, 33, 101617.

[4] Zhong, R., & Wille, K. (2018). Influence of matrix and pore system characteristics on the durability of pervious concrete. Construction and Building Materials, 162, 132–141.

[5] Wu, Y., Dai, J., Shi, B., et al. (2022). The strength and elastic modulus of pervious concrete considering pore and fiber during freeze–thaw cycles. Sustainability, 14(23), 16217.

[6] Wu, F., Yu, Q., & Brouwers, H. J. H. (2022). Mechanical, absorptive and freeze–thaw properties of pervious concrete applying a bimodal aggregate packing model. Construction and Building Materials, 333, 127445.

[7] Zhang, G., Wang, S., Wang, B., et al. (2020). Properties of pervious concrete with steel slag as aggregates and different mineral admixtures as binders. Construction and Building Materials, 257, 119543.

[8] Zhao, H., Geng, Q., & Liu, X. (2023). Influence of freeze–thaw cycles on mechanical properties of pervious concrete: From experimental studies to discrete element simulations. Construction and Building Materials, 409, 133988.

[9] Berto, L., Saetta, A., & Talledo, D. (2015). Constitutive model of concrete damaged by freeze–thaw action for evaluation of structural performance of RC elements. Construction and Building Materials, 98, 559–569.

[10] Qiu, J., Zhou, Y., Vatin, N. I., et al. (2020). Damage constitutive model of coal gangue concrete under freeze-thaw cycles. Construction and Building Materials, 264, 120720.

[11] Lemaitre, J. (1985). A continuous damage mechanics model for ductile fracture.

[12] Weibull, W. (1951). A statistical distribution function of wide applicability. Journal of Applied Mechanics.